Interdiffusion in CoFe/Cu multilayers and its application to spin-valve structures for data storage

Erik B. Svedberg[a)] and Kent J. Howard
Seagate Technology, Pittsburgh, Pennsylvania 15222-4215

Martin C. Bønsager and Bharat B. Pant
Seagate Technology, Bloomington, Minnesota 55435-5489

Anup G. Roy and David E. Laughlin
Department of Electrical and Computer Engineering, Carnegie Mellon University, Pittsburgh, Pennsylvania 15213-3890

Spin-valve structures might be exposed to higher temperatures in future disk drive applications and might thus degrade faster than it does today if proper materials and methods are not used. In order to determine whether this degradation is due to interdiffusion between constituent layers or is dominated by other phenomena, the interdiffusion coefficients for all layers in the spin valve have to be determined. For diffusion driven degradation it would then be possible to predict lifetimes based on a maximum allowed reduction in $\Delta R/R$ where R is the resistivity. Here we report the initial results for a CoFe/Cu interface, common to many spin-valve structures. Interdiffusion in (111) textured polycrystalline CoFe/Cu multilayers has been measured and quantified by x-ray reflectometry. Bulk diffusion is dominant at temperatures above $\sim 540\,°C$ and is described by an activation energy of $E_a = 2.41\,eV$ and a prefactor of $D_0 = 2.92 \times 10^{-8}\,m^2/s$. Below temperature of 540 °C grain boundary diffusion dominates and is characterized by $E_a = 0.90\,eV$ and $D_0 = 1.91 \times 10^{-17}\,m^2/s$. Prior to stabilization of the diffusion process there is an initial rapid change in the (111) texture. During initial ''sharpening'' of the CoFe/Cu multilayer interfaces there is shortening of the periodicity as well as a decrease in out-of-plane lattice spacing. © *2003 American Institute of Physics.* [DOI: 10.1063/1.1586479]

I. INTRODUCTION

It is generally accepted that the giant magnetoresistance (GMR) effect originates in spin-dependent scattering, i.e., different scattering rates for spin-up and spin-down electrons. In Fe/Cr layers, for instance, it is agreed upon both experimentally[1] and theoretically[2] that by far the most important contribution to the GMR effect is due to spin-dependent scattering at the Fe/Cr interfaces. The role of the interfaces is, however, much less clear in the Co/Cu system. Nevertheless, it is important to know the interface structure and how it reacts to elevated temperatures. In this article we study the interdiffusion of CoFe/Cu interfaces, a common interface in spin valves, in the form of a multilayer.

From a scientific point of view the diffusion mechanisms in many multicomponent systems are still poorly understood, and knowledge of the diffusion data and mechanisms is highly desirable to understand the physical properties and phenomena in multilayers. From a technological viewpoint, knowledge of the diffusion is an important prerequisite for application of multilayers in fields such as data storage. Despite many years of effort, the diffusivity in multilayers has remained poorly quantified. This is because of the difficulty in measurement associated with low diffusivity (less than $10^{-23}\,m^2/s$) in thin films at low annealing temperatures. One of the most sensitive techniques for measuring interdiffusion is by modulated film, i.e., the use of multilayer structures and the study of the decay of satellite peaks in x-ray reflectometry[3–5] even though other techniques are emerging such as the use of transmission electron microscopy (TEM) and imaging filtering.[6] The theory of interdiffusion in artificial compositionally modulated materials is well developed, and in its simplest form, the equations are linearized by treating several parameters as composition independent.[7] This is the most sensitive technique available for measuring diffusivities as low as $10^{-27}\,m^2/s$ in multilayers with modulation period of a few nanometers. For a detailed description of the diffusion equations see the paper ''Diffusion in $Co_{90}Fe_{10}/Ru$ Multilayers'' by the same authors in this issue, and Refs. 8–10.

II. EXPERIMENT

Multilayers of Co_xFe_{1-x}/Cu with $x \sim 0.9$ were deposited by magnetron sputtering from 100 mm diam compound targets in 4 – 5 mTorr Ar gas with a throw distance of 200 mm. The CoFe thickness was 3.5 nm and the Cu thickness 2.5 nm. The bilayer was repeated 25 times and capped with a 3 nm Al_2O_3 layer. The substrates were 3 in. Si wafers with a 100 nm SiO_2 layer and a 5 nm $(Ni_{80}Fe_{20})_{60}Cr_{40}$ seed. The multilayer structures were subsequently annealed in a rapid thermal annealer (RTA) at temperatures ranging from 490 to

a)Electronic mail: e_svedberg@yahoo.com

600 °C and times from 7 min to 18 h. The RTA employs quartz lamps for heating and the temperature is controlled by a calibrated pyrometer.

The annealed samples were analyzed with x-ray reflectometry to determine the degree of interdiffusion, described in Sec. I. Furthermore, transmission electron microscopy cross sections were used to determine the microstructure in the samples. A JEOL JEM 2000-EXII and a Philips TECNAI F20 were used for this. Auger depth profiling during Zalar rotation was employed to verify the degree of intermixing and chemical composition. A Physical Electronics 660 scanning Auger microprobe was used under the following conditions: electron beam at 10 keV, 1 μA, tilted 30° from the sample normal. The ion beam conditions were 3 keV Ar$^+$, 2.0 μA, applied in a 7 mm^2 raster. The resulting sputter rate was 1.1 nm/min for the depth profiling.

III. RESULTS

Auger data in Figs. 1(a)–1(c) indicate that there seems to be a slight deficiency of Fe in the Co$_x$Fe$_{1-x}$ layers from x ∼0.9. Although there is interference between Co and Fe that necessitates the use of a second Fe peak the deficiency is too large to be accounted for by interference alone. Similar interference exists between Cu and Co that might cause the Co values to be slightly too high for the atomic concentration reported. However, the Cu line is totally free of interference and as such is the best absolute indicator of quantitative concentration and diffusion. The samples annealed for 7 min [Fig. 1(b)] and 1 [Fig. 1(c)] indicate from the Auger data that oxygen is not present anywhere in the samples at any elevated levels. Auger depth profiles of the oxygen and Al peaks indicate that the annealing at 575 °C does not move or diffuse the Al from the Al$_2$O$_3$ cap. The oxygen levels are above the background level only in the first 5 nm (the cap) in the as-deposited samples, and, after 1 h of annealing, only the first 17 nm has elevated oxygen levels. (17 nm is only a small fraction compared to the total film thickness of 150 nm.) Since the background level of oxygen does not change it is safe to conclude that there is no significant oxidation of the CoFe/Cu multilayer.

However, the annealed samples show a Cr signal for the first 5 nm after 7 min of annealing time and 10 nm for the sample heated for 1 h. This Cr signal is not present in the as-deposited sample. Scanning electron microscopy (SEM) data in Figs. 2(a)–2(c) show images of the surface of the as-deposited film, a film annealed at 575 °C for 7 min and a film annealed at 575 °C for 1 h. The as-deposited film appears smooth and featureless at this level of magnification. Annealing for 7 min or 1 h produces 1.6 μm size "bumps" that cover 3.8% of the surface. Even though most of these have already appeared after 7 min of annealing there is an increase in coverage after 1 h to 8.3%. Figures 3(a) and 3(b) show 1×1 μm^2 atomic force microscopy (AFM) images of the in SEM "smooth," surfaces of an as-deposited film and a film annealed at 575 °C for 1 h. The surface features in both images have lateral size of ∼50 nm. The root mean square surface roughness increases slightly as the film is annealed from ∼0.6 nm as deposited to ∼0.8 nm after 1 h at 575 °C.
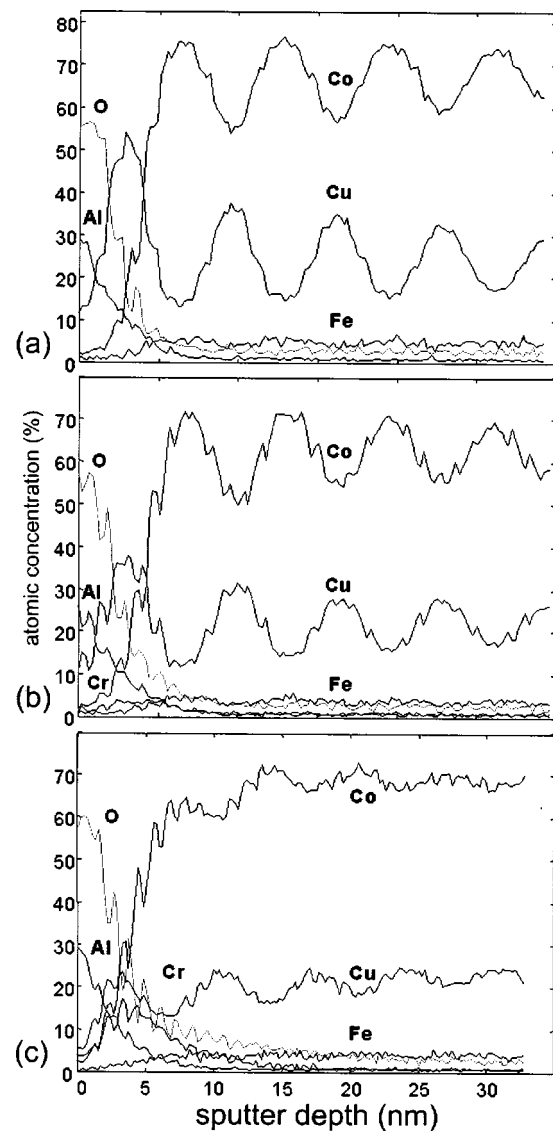

FIG. 1. Auger depth profiling during Zalar rotation for (a) the as-deposited film, (b) a film annealed at 575 °C for 7 min and (c) a film annealed at 575 °C for 1 h. A Physical Electronics 660 scanning Auger microprobe was used under the following conditions: electron beam at 10 keV, 1 μA, tilted 30° from the sample normal. The ion beam conditions were 3 keV Ar$^+$, 2.0 μA, applied in a 7 mm^2 raster. The resulting sputtering rate was 1.1 nm/min.

The size of the surface features corresponds to the size of the grains in the TEM images in Fig. 4(a)–4(c). Figures 4(a) and 4(b) show that each grain boundary has a small cusp on the surface and that the grains are otherwise relatively smooth on the surface. The as-deposited multilayer structure in Fig. 4(a) is possible to see even though there appears to be a large amount of strain and other contrast mechanisms present. Figure 4(b) shows the multilayer structure after a 7 min anneal at 575 °C; here the multilayer period can clearly be made out. In Fig. 4(c), multilayer periodicity is almost completely gone after a 1 h anneal at 575 °C.

Figure 5 shows high angle 2θ x-ray diffraction data for the as-deposited film, a film annealed at 575 °C for 7 min and a film annealed at 575 °C for 1 h. The shift in the center multilayer peak at ∼44° 2θ indicates a decrease in average out-of-plane lattice parameter spacing. The average period is,

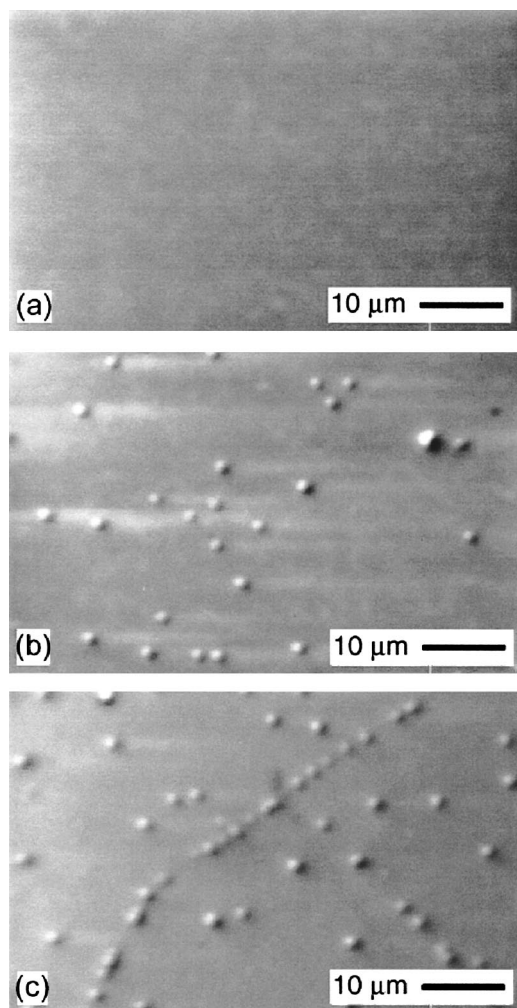J. Appl. Phys., Vol. 94, No. 2, 15 July 2003

Svedberg *et al.*   1003

FIG. 2. SEM images of the surface of (a) the as-deposited film, (b) a film annealed at 575 °C for 7 min and (c) a film annealed at 575 °C for 1 h.

FIG. 3. 1×1 μm^2 AFM images of film (a) as deposited and (b) annealed at 575 °C for 1 h.

for example, 6.50 ± 0.01 nm after 7 min of annealing and 6.42 ± 0.01 nm after 21 min. The other peaks surrounding the main peak [Figs. 5(a) and 5(b)] are superlattice peaks that are a result of the 6 nm periodic CoFe/Cu multilayer structure. The highest peak intensity is from the sample annealed for 7 min. Figure 6 shows the rocking curves for the main peak in Fig. 5, as expected the 7 min anneal shows the highest intensity. However, it also has the smallest full width at half maximum (FWHM) of 3.4° θ compared to 7.6° for the as-deposited sample and 6.8° for the sample heated for 1 h. The FWHM value indicates the spread in the surface normal of the planes parallel to the film surface, i.e., the mosaicity of the crystallographic orientation of the film.

Figure 7 shows $\omega - 2\theta$ x-ray reflectometry data for the as-deposited film as well as for films annealed at 575 °C for 30 min and 1, 2 and 4 h. The scan clearly shows the first satellite peak at 1.56° 2θ slowly decreasing in height for all samples except the one annealed for 4 h where the peak has almost the same height as the background noise. This is the peak used in the diffusivity calculations. The scans also show a weak indication of a second satellite peak at 2.85° 2θ for the as-deposited sample and the one annealed for 30 min. Figure 8 shows $\omega - 2\theta$ x-ray reflectometry data in the region
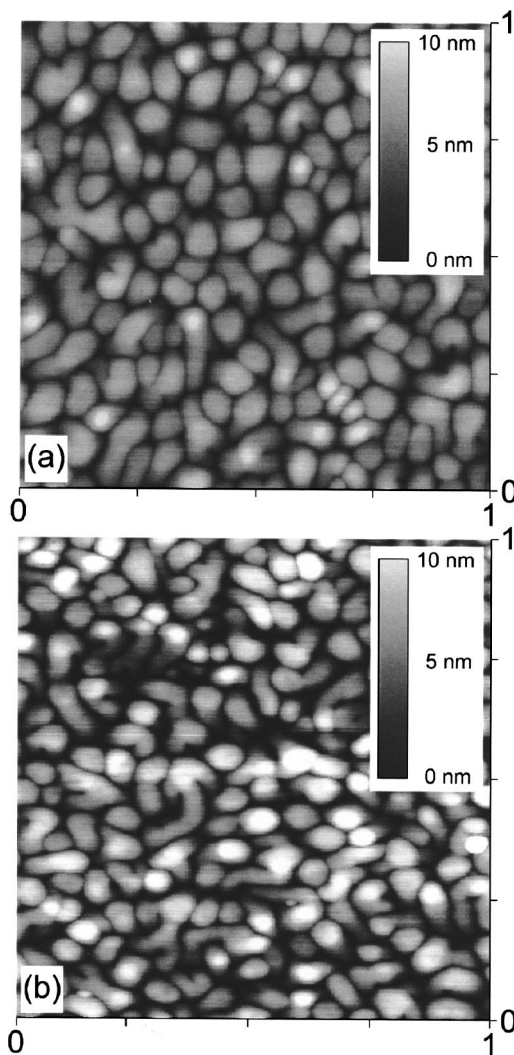
around the second peak for the as-deposited film as well as for films annealed at 575 °C for 7, 14, 21 and 30 min. The scans clearly show a second satellite peak at 2.85° 2θ for the samples annealed for 7, 14 and 21 min.

Figure 9 shows the intensity of the first x-ray reflectometry peak normalized to the intensity prior to annealing at 575 °C. There is an initial nonlinear portion during the first 3000 s where after interdiffusion progresses "linearly" in the log–lin plot. In Fig. 10 the linear portion of Fig. 9 is shown together with similar data from samples annealed at temperatures of 490, 505, 520, 550, 560, and 600 °C as well. The annealing times varied from 0.2×10^4 to 6.6×10^4 seconds. Each slope represents a different diffusion rate. In Fig. 11 the diffusion rates are plotted in an Arrhenius plot. There is one change in diffusion rate with temperature above ~ 540 °C which is described by an activation energy of $E_a = 2.41$ eV and a prefactor of $D_0 = 2.92 \times 10^{-8}$ m^2/s. Below ~ 540 °C interdiffusion is characterized by $E_a = 0.90$ eV and $D_0 = 1.91 \times 10^{-17}$ m^2/s.

IV. DISCUSSION

Theoretically the Auger data of a perfect multilayer without mixing the concentration of Cu should change from

FIG. 5. High angle x-ray diffraction data for (a) the as-deposited film, (b) a film annealed at 575 °C for 7 min and (c) a film annealed at 575 °C for 1 h. The shift in the peak at 44 ° indicates a decrease in out-of-plane lattice parameter spacing.
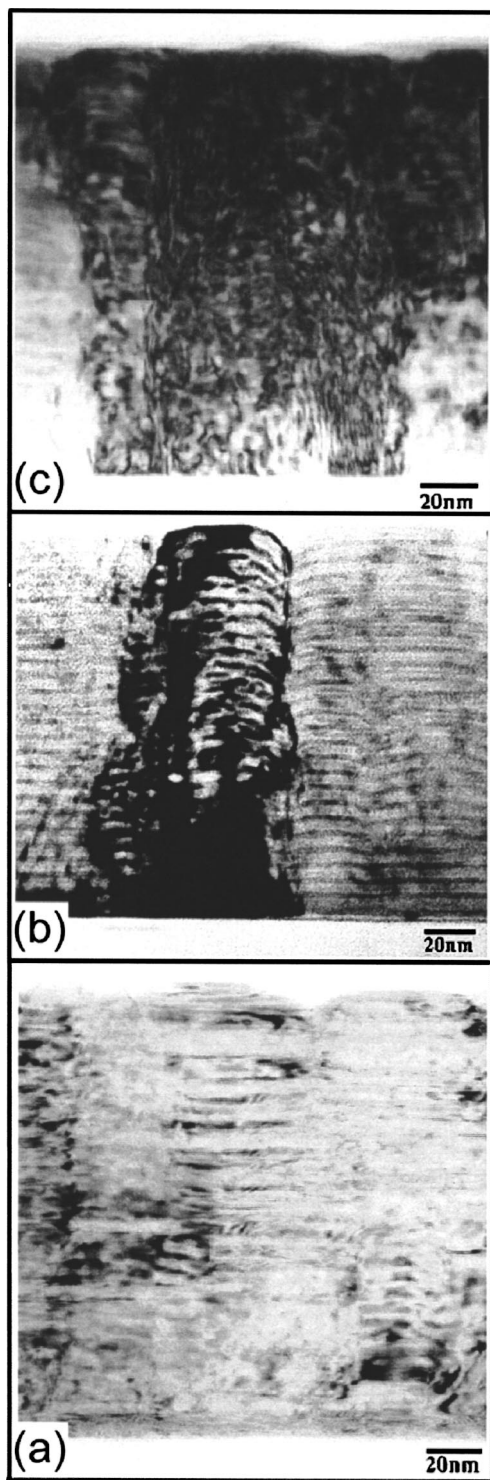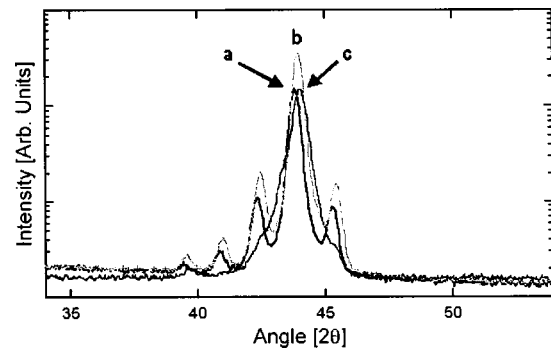

FIG. 4. TEM images of the surface of (a) the as-deposited film, (b) a film annealed at 575 °C for 7 min and (c) a film annealed at 575 °C for 1 h.

0% to 100% and the CoFe signals should represent the missing part of the total concentration. However, during the Auger measurement the signal is averaged over an area that has intrinsic roughness from both the surface as well as from the milling process. This roughness results in a mixing of signals from adjacent layers and thus a Cu signal that instead changes from 15% to 40% in the as-deposited film. That is also why it is difficult to use Auger data to analyze the dif-

fusion process with high accuracy. The Auger data also show a Cr peak appearing at the surface with annealing. This Auger peak coincides with small 1 μm bumps that appear in the SEM images of the films. The Cr peaks extension is only for the first 10 nm of the film structure after which the Cr signal goes well below the 0.5% level in the multilayer. The only source of Cr comes from the 5 nm thick NiFeCr seed deposited prior to the CoFe/Cu multilayer. We believe that the Cr diffuses through the grain boundaries in the structure and causes the bumps at the surface seen in the SEM images during the initial stages of annealing of these samples. We also believe that this process is responsible for part of the initial nonlinear behavior in diffusion, as seen in Fig. 9. However, as annealing progresses the Cr segregation reaches an equilibrium and slower CoFe/Cu diffusion is seen.

The fact that the grain boundaries in the TEM images can safely be correlated to the surface features in the AFM images makes it possible to estimate the grain boundary area in these films. From the actual length of the network of cusps seen in the AFM images it is possible to estimate the grain boundary area as $5.2\times10^6\pm0.4\times10^6$ nm^2 for each μm^3. This is valid if the grains are estimated to be prisms of 150 nm height.
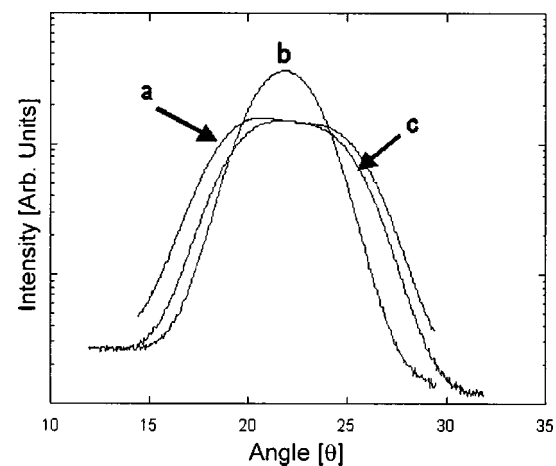

FIG. 6. X-ray diffraction rocking curves on (a) the as-deposited film, (b) a film annealed at 575 °C for 7 min and (c) a film annealed at 575 °C for 2 h.
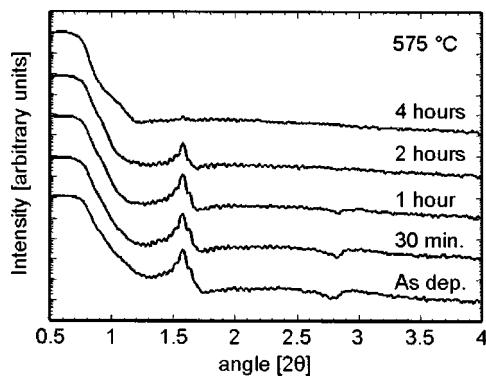
FIG. 7. X-ray reflectometry scans of samples annealed at 575 °C for 0, 0.5, 1, 2, and 4 h.

FIG. 9. Initial nonlinear behavior of interdiffusion. Displayed are x-ray diffraction intensity data. The intensity, I, is normalized to the unannealed sample intensity, I_0, prior to annealing. The temperature was 575 °C. The annealing times varied from 400 to 1.5×10^4 s.

The decrease in average multilayer period (from 6.50 ± 0.01 nm after 7 min of annealing to 6.42 ± 0.01 nm after 21 min), together with a initial reduction in the FWHM of the x-ray data indicate initial relaxation of the film to a less stressed state with a better defined multilayer structure. This can also be seen in the TEM images where Fig. 4(b) shows a distinct multilayer that is better defined than the as-deposited sample. Further support for a better defined multilayer after a short initial annealing is found in the $\omega - 2\theta$ x-ray reflectometry data. In the diffraction data the second satellite peak appears temporarily for the films annealed at 575 °C for 7, 14 and 21 min. This behavior can be explained by the fact that Cu does not mix with CoFe so initially the interfaces become more abrupt as the elements separate into a more sharply layered structure and the second superlattice peak appears in the x-ray spectra. The initial interface roughness comes from ballistic intermixing during the sputtering process. Binary alloy phase diagrams[11] indicate that there can be up to 0.4 at. % Cu in Co at equilibrium, and at low temperature Fe precipitates from a Cu matrix at 2.7 at. % Fe. However, as annealing progresses diffusion degrades the overall uniformity of individual CoFe and Cu layers, thus reducing the abruptness of the interfaces in the multilayer, especially that averaged over the sampling area of the x-ray diffractometer, which is several mm^2. There are, at least, two ways compositional modulation can be destroyed in a multilayer:

either the layers mix and form a new alloy or they separate into irregular regions and essentially destroy the modulation. Work by Bobeth *et al.*[12] has shown that annealing to temperatures where a Co/Cu multilayer has its periodicity destroyed produces a two phase mixture in which small irregularly shaped Cu and Co phase regions are dominant. Figure 9 shows the intensity of the first x-ray reflectometry peak normalized to the intensity prior to annealing at 575 °C. There is an initial nonlinear portion of approximately 3000 s (~ 50 min). During this the multilayer undergoes sharpening of the interface as well as fast diffusion of Cr to the surface and a reduction in stress. After the initial period diffusion progresses "linearly" in the log–lin plot of Fig. 9. In Fig. 10 the linear portion of Fig. 9 is shown together with similar data from samples annealed at temperatures of 490, 505, 520, 550, 560, and 600 °C as well. This temperature range is suitable for detecting decay of the first superlattice peak in x-ray reflectometry scans. (The noise floor is at $\sim I/I_0 = 0.008$ in this case and temperatures lower than 490 °C give too long annealing times.) Since each slope represents a different diffusion rate it is possible to generate the Arrhenius plot in Fig. 11 where the diffusion constant is plotted vs $1/T$. For temperatures higher than ~ 540 °C, the diffusion con-
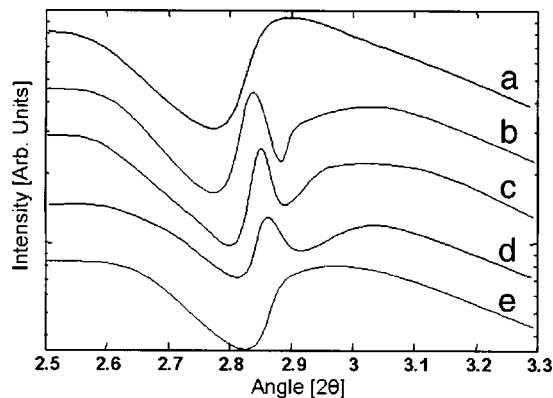

FIG. 8. X-ray reflectometry scans of samples annealed at 575 °C for (a) 0, (b) 7, (c) 14, (d) 21, and (e) 30 min. The data were fit to a spline function to clarify the peaks.
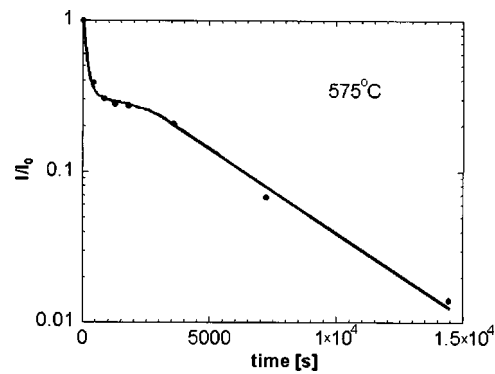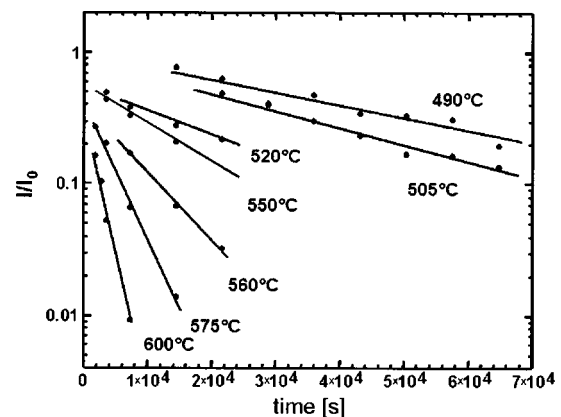

FIG. 10. X-ray diffraction intensity data for different annealing times and temperatures. The intensity, I, is normalized to the unannealed sample intensity, I_0, prior to annealing. The temperatures were 490, 505, 520, 550, 560, 575, and 600 °C. The annealing times varied from 0.2×10^4 to 6.6×10^4 s.
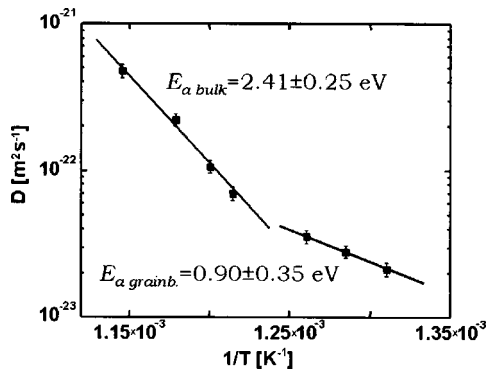
FIG. 11. Interdiffusion data for the CoFe/Cu system in an Arrhenius plot where the diffusion rates are plotted vs $1/T$. There is one change in diffusion rate with temperatures above $\sim 540\,°C$ which is described by an activation energy of $E_a = 2.41 \pm 0.25$ eV and a prefactor of $D_0 = 2.92 \times 10^{-8}$ m^2/s. Below $\sim 540\,°C$ diffusion is characterized by $E_a = 0.90 \pm 0.35$ eV and $D_0 = 1.91 \times 10^{-17}$ m^2/s.

stant is characterized by an activation energy of $E_a = 2.41 \pm 0.25$ eV and a prefactor of $D_0 = 2.92 \times 10^{-8}$ m^2/s. Below $\sim 540\,°C$ the diffusion is characterized by $E_a = 0.90 \pm 0.35$ eV and $D_0 = 1.91 \times 10^{-17}$ m^2/s. These two different activation energies represent bulk diffusion and the diffusion of atoms through the grain boundaries, respectively. It is well established that the mean jump frequency in a grain boundary-type defect is much higher than that in the crystal lattice and, hence, the diffusivity is higher in these regions.[13] The activation energy for bulk diffusion fits well solute tracer diffusivity data of Cu–Fe and Cu–Co systems. The activation energy for the Cu–Co system was 2.3–2.4 eV and for the Cu–Fe system it was 2.2 eV.[14] One would expect that the activation energy for the alloy system would not be too far from that of its constituents and would perhaps be closer to the Co value since the alloy is CoFe with 90% Co. It should also be pointed out that the data from the multilayer structures here are averages of CoFe/Cu and Cu/CoFe interfaces. These interfaces can be mixed differently during deposition due to the differences in sputter energies pointed out in Ref. 15 for Co/Ru and Ru/Co and calculated for Mo/W and W/Mo in Ref. 16. There is also other work where an activation energy is determined directly for changes in the magnetoresistance signal, such as in the work by Bal *et al.*[17] where it was determined for Co/Cu/Co stacks.

V. CONCLUSIONS

The dimensions of spin-valve structures are constantly being reduced, and might be exposed to higher temperatures in some disk drive applications, thus, they are subject to the risk of thermal decay. In order to determine the degradation it is important to know the interdiffusion coefficients for all layers in the spin valve. Here we reported initial results from a multilayer system containing a CoFe/Cu interface common to many spin-valve structures. Interdiffusion in (111) textured polycrystalline CoFe/Cu multilayers was measured and quantified by x-ray reflectometry. Bulk diffusion is dominant at temperatures above $\sim 540\,°C$ and is described by an activation energy of $E_a = 2.41$ eV and a prefactor of $D_0 = 2.92$

$\times 10^{-8}$ m^2/s. Below 540 °C grain boundary diffusion dominates and is characterized by $E_a = 0.90$ eV and $D_0 = 1.91 \times 10^{-17}$ m^2/s. From TEM and AFM images it was possible to estimate the grain boundary area as $5.2 \times 10^6 \pm 0.4 \times 10^6$ nm^2 for each μm^3 in the samples used in this study. Prior to stabilization of the diffusion process there is an initial rapid change in the (111) texture and it becomes sharper and more defined along the surface normal. At 575 °C the crystallographic change in texture goes from a full width half maximum of 7.5° to 3.7°. Upon further annealing the full width half maximum reverts back to a value of $\sim 6.4°$ as the diffusion process progresses. During initial sharpening of the CoFe/Cu multilayer interfaces there was shortening of the periodicity as well as a decrease in out-of-plane lattice spacing. Cross sectional TEM images of the multilayers, at different stages of annealing, initially showed a strained film in which individual CoFe/Cu layers were not visually so well defined; they also showed the film to initially reduce the strain and sharpen the interfaces. As interdiffusion proceeds the TEM images lose resolution of the multilayer structure in the films. This transient behavior can be explained by the fact that Cu does not mix well with CoFe at equilibrium, so initially the interfaces become more abrupt as the elements separate from their sputtering process-induced intermixing, and stress is generally reduced in the film. As the interdiffusion process continues degradation of the multilayer structure becomes apparent and it was quantified.

ACKNOWLEDGMENT

[1] E. E. Fullerton, D. M. Kelly, J. Guimpel, I. K. Schuller, and Y. Bruynseraede, Phys. Rev. Lett. **68**, 859 (1990).
[2] A. Oguri, Y. Asano, and S. Maekawa, J. Phys. Soc. Jpn. **61**, 2652 (1992).
[3] R. J. Borg and G. J. Dienes, An Introduction to Solid State Diffusion (Academic, Boston, 1988).
[4] H. E. Cook and J. E. Hilliard, J. Appl. Phys. **40**, 2191 (1969).
[5] M. P. Rosenblum and D. Turnbull, Appl. Phys. Lett. **37**, 184 (1980).
[6] R.-T. Huang, F.-R. Chen, J.-J. Kai, I.-F. Tsu, S. Mao, and W. Kai, J. Appl. Phys. **89**, 7625 (2001).
[7] A. L. Greer and F. Spaepen, in Synthetic Modulated Structures, edited by L. L. Chang and B. C. Geissen (Academic, New York, 1985).
[8] J. DuMond and J. P. Youtz, J. Appl. Phys. **11**, 357 (1940).
[9] A. Guinier, X-ray Diffraction (Freeman, San Francisco, 1963).
[10] T. Tsakalakos, Ph.D. thesis, Northwestern University, Evanston, IL, 1977.
[11] Binary Alloy Phase Diagrams, Ver. 1.0, 2nd ed. with updates on CD-ROM (ASM International, Metals Park, OH, 1996).
[12] M. Bobeth, M. Hecker, W. Pompe, C. M. Schneider, J. Thomas, A. Ullrich, and K. Wetzig, Z. Metallkd. **92**, 810 (2001).
[13] P. G. Shewmon, in Series in Material Science and Engineering, edited by M. B. Bever (McGraw–Hill, New York, 1963).
[14] D. B. Butrymowicz, J. R. Manning, and M. E. Read, International Copper Research Association Monograph V. The Metallurgy of Copper. Diffusion Rate Data and Mass Transport Phenomena for Copper Systems (National Bureau of Standards, Washington, DC, 1977); D. B. Butrymowicz, International Copper Research Association Monograph VIII. The Metallurgy of Copper, Diffusion Rate Data and Mass Transport Phenomena for Copper Systems (National Bureau of Standards, Washington, DC, 1981).
[15] K. Bal, H. A. M. van den Berg, D. Deck, and Th. Rasing, J. Appl. Phys. **90**, 5228 (2001).
[16] E. B. Svedberg, J. Birch, I. Ivanov, P. Münger and J.-E. Sundgren, J. Vac. Sci. Technol. A **16**, 633 (1998).
[17] K. Bal, H. A. M. van den Berg, A. Keen, and Th. Rasing, J. Appl. Phys. **89**, 7508 (2001).